

LIFETIMES AND FINE STRUCTURE OF THE METASTABLE AUTOIONIZING $(1s2s2p)^4P_J$ STATES OF THE NEGATIVE HELIUM ION*

L. M. Blau, R. Novick, and D. Weinflash

Physics Department, Columbia University, New York, New York 10027
(Received 27 April 1970)

The decay of the differentially metastable autoionizing $(1s2s2p)^4P_J$ states of the $^4\text{He}^-$ ion has been studied by time-of-flight techniques in an axial magnetic field, and Zeeman quenching has been observed. Two distinct lifetime components (11 μsec , 210 μsec) have been identified in a 100-eV beam with an axial field of 400 G. The zero-field lifetimes obtained from these and other measurements are $11 \pm 5 \mu\text{sec}$ for $J = \frac{1}{2}, \frac{3}{2}$, and $345 \pm 90 \mu\text{sec}$ for $J = \frac{5}{2}$. The $\frac{5}{2} - \frac{3}{2}$ fine-structure interval is estimated to be $0.050 \pm 0.015 \text{ cm}^{-1}$.

The electron affinity of helium was first considered by Wu¹ in 1936 and a negatively charged state of helium was observed by Hilby² in 1939 using a mass spectrometer. Other experimental work³⁻⁴ established that He^- could be produced by charge-exchange collisions. Holøien and Midtdal⁵ employed a four-term variational wave function to calculate the energy of the $(1s2s2p)^4P_J$ states and pointed out that these states would be metastable against direct Coulomb autoionization. Although more careful computation revealed that the four-term wave function did not in fact lead to a positive electron affinity for the $(1s2s)^3S$ state, Holøien and Geltman⁶ found that a 30-term wave function gave an electron affinity $E_A \geq 0.033 \text{ eV}$. Brehm, Gusinow, and Hall⁷ measured the electron affinity via laser photodetachment, obtaining a value $E_A = 0.080 \pm 0.002 \text{ eV}$.

It was realized that the 4P_J states could decay to the He^0 ground state plus a free electron by spin-dependent interactions. Each J level would have a different lifetime and an external magnetic field would quench the longest-lived $J = \frac{5}{2}$ state by mixing it with other states of the same multiplet. These predictions were experimentally verified for the corresponding 4P_J states in lithium.⁸ Dips in the Zeeman quenching curve which result from anticrossing levels enabled the determination of the fine-structure intervals and lifetimes for each J state. Various authors⁹⁻¹² have calculated the lifetime of the $^4P_{5/2}$ state for atoms in the isoelectronic series, obtaining values for He^- ranging from 1700 to 266 μsec . Since the $^4P_{5/2}$ state can decay only via the tensor spin-spin interaction, there is no ambiguity concerning the operator in the matrix element for the transition. Hence the wide range of theoretical values implies that the He^- lifetime is highly sensitive to the precise form of the wave functions used for the initial and final states. The theoretical lifetime increases when the initial state is described by a superposition of Hartree-

Fock configurations instead of a single $(1s2s2p)$ configuration. The electron correlation implicit in the more complicated initial wave function increases the average interelectron separation, thereby reducing the effectiveness of the spin-spin interaction in causing the decay. On the other hand, the theoretical lifetime decreases when the final state includes the polarization of the $(1s^2)$ He^0 ground state by the ejected electron and the consequent distortion of the continuum wave function of the ejected electron by the polarized atom (see Table I). There are at least two physical arguments that can be given for this shortening of the lifetime. First, the induced multipoles in the atom produce an attractive potential which serves to increase the density of the ejected electron in the vicinity of the atom, thereby increasing the interaction. Second, the induced multipoles themselves tend to increase the overlap of the final state of the atom with the initial state. A reliable experimental value for the lifetime is needed to evaluate the different theoretical approaches and the approximations made in the calculations.

We report herein the preliminary results of an experiment which establishes that the $J = \frac{5}{2}$ lifetime is $345 \pm 90 \mu\text{sec}$ and that a weighted average of the $J = \frac{3}{2}$ and $J = \frac{1}{2}$ lifetimes is 11 μsec . The $\frac{5}{2}$ -

Table I. Theoretical values for the lifetime of the $(1s2s2p)^4P_{5/2}$ state of He^- (in μsec).

		No. of configurations in initial-state wave function	
		$N=1$	$N=28$
Polarization of the final state included	No	303 ^a	550 ^a
	Yes	266 ^b	455 ^c
Present experimental value		345 \pm 90 ^d	

^aRef. 10. ^bRef. 12. ^cRef. 15. ^dPresent work.

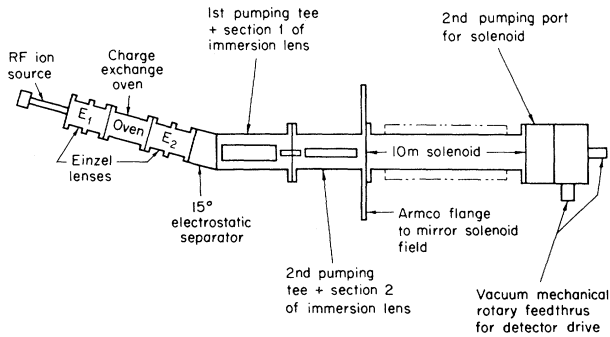


FIG. 1. Schematic diagram of the He^- source and detection regions.

$\frac{3}{2}$ fine-structure interval is estimated to be $0.050 \pm 0.015 \text{ cm}^{-1}$.

In our investigation, we prepare a beam of He^- by double charge exchange, a technique proposed by Donnally.¹³ A schematic representation of our apparatus is shown in Fig. 1. A 3000-eV He^+ beam is extracted from an rf discharge and passes through a potassium vapor where it suffers two collisions with neutral potassium atoms. The first collision results in a charge exchange and produces the metastable $(1s2s)^3S$ state of He^0 . The second collision results in another charge exchange and produces the desired He^- state. The potassium vapor density can be varied to maximize the production of He^- , and negative-ion currents of 100 nA are easily obtained. The beam emerging from the potassium vapor is electrostatically separated into its charge components and the total positive beam is collected as a monitor on beam stability. The He^- beam is deflected into a series of electrostatic lenses and decelerated to any desired energy above 50 eV. The beam then passes into a 10-m drift-tube solenoid wound to provide axial magnetic fields up to 1500 G. The ion source and detection regions are separated by a differential pumping aperture. The pressure on the source side is 3×10^{-6} Torr when gas is admitted to the rf discharge, while the pressure in the detection region, which is pumped at either end by 4-in. mercury diffusion pumps, is at least an order of magnitude lower. The He^- beam is detected by a Faraday cup which is movable in the vacuum chamber nearly the full length of the drift tube. A high-transparency grid, electrically insulated from the Faraday cup, is placed across the entrance of the detector. When the negative bias on the grid is greater than 20 V, the 19.7-eV electrons produced in the beam by autoionization of He^- cannot enter the detector and the current recorded

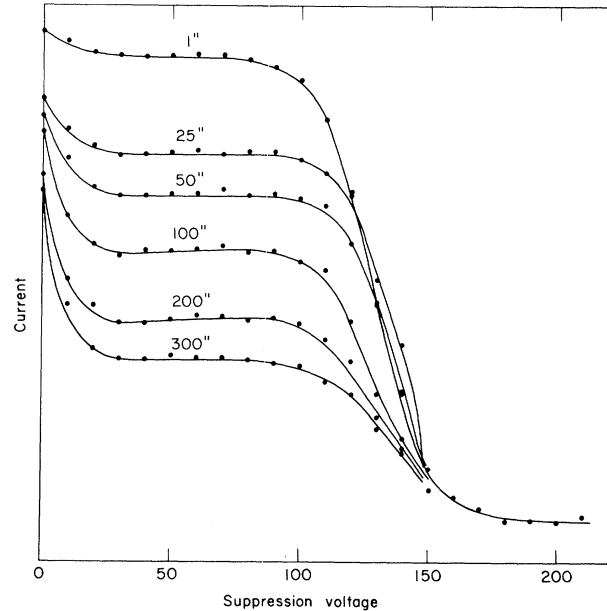


FIG. 2. Current reaching the movable Faraday cup at successive detector positions as a function of negative suppression voltage. Note the buildup of the low-energy component and the decrease of the high-energy component as the detector is moved away from the source.

is due to He^- alone.

Figure 2 shows typical experimental results for suppression of a 150-eV He^- beam. The graphs are Faraday-cup currents versus suppression voltage at successive positions of the detector. The development with increasing distance of the feature below 25 V is evidence of the buildup of electrons in the beam, a confirmation that we are observing autoionization in flight. The sum of He^- and e^- currents at zero suppression is not independent of detector position as would be expected from conservation of charge because half the electrons are ejected backwards and hence are lost to our detector.

Data runs were taken at magnetic fields between 400 and 1500 G to directly observe differential metastability and Zeeman quenching. The residual pressure in the vacuum system was varied over a range from 2×10^{-7} to 3×10^{-6} Torr by regulating the water flow in the cooling lines of the solenoid. For all pressures and fields, the graph of He^- current versus distance could be fit to better than 1% by a sum of two exponentials. In Fig. 3, a run for a 100-eV He^- beam at a field of 400 G and a residual pressure of 2×10^{-7} Torr is fitted with lifetime components of 10.2 and 161 μsec . The 1% accuracy of the fit to individual runs is not reflected in a corresponding

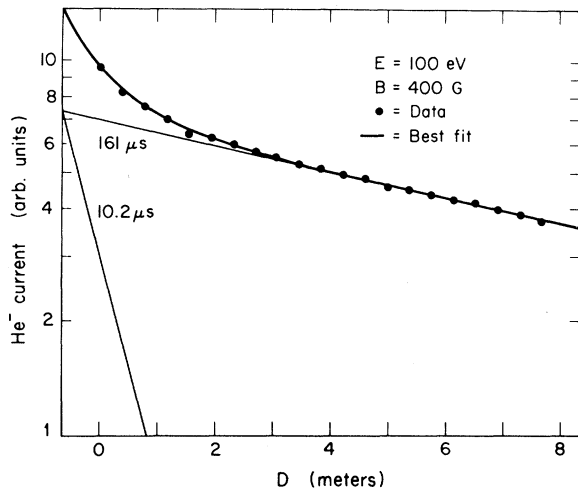


FIG. 3. Typical He⁻ data run fitted by a sum of two exponentials. The two components have equal weight when extrapolated back to the source, which is located at $D = -1.2$ m.

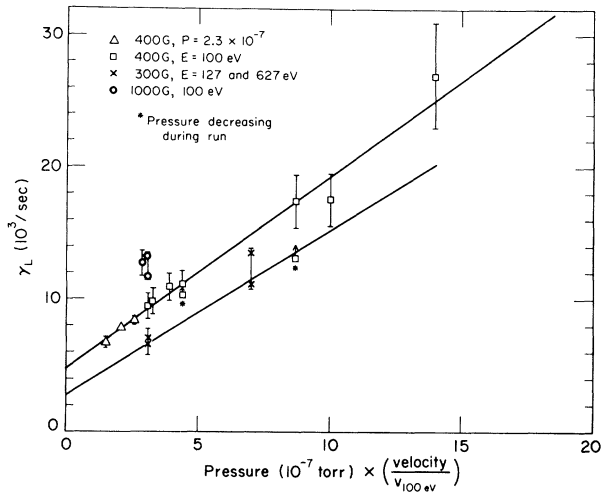


FIG. 4. The decay constant of the long-lived He⁻ component γ_L as a function of pressure times velocity at several magnetic fields.

accuracy in the final result for the lifetimes because of uncontrolled changes in the residual gas pressure and beam intensity during individual runs. The closest position of the detector to the He⁻ source corresponds to a flight time of 7 μ sec for a 100-eV beam. If the observed relative weights of the two components are extrapolated back to the source, the weights at production are equal. The decay rate of a particular component in a given magnetic field is $\gamma_{\text{observed}} = \gamma_{\text{natural}} + n\sigma v$, where n = residual gas number density, v = beam velocity, and σ = the total cross section for removing He⁻ from the beam by either collisional quenching or large-angle scattering. Extrapolation of γ_{observed} to zero residual pressure was accomplished by separately varying the velocity and pressure. Figure 4 shows the dependence of the longer component γ_L on the product $p v$. The agreement between the two methods of extrapolation is shown by the collinearity of the triangles and squares in Fig. 4. The zero-pressure decay rates of the two components at $H = 400$ G are $(4.8 \pm 0.3) \times 10^3 \text{ sec}^{-1}$ and $(9 \pm 1) \times 10^4 \text{ sec}^{-1}$. The corresponding lifetimes are 210 and 11 μ sec. Insufficient data were obtained to make reliable pressure extrapolations for other magnetic fields. At higher fields, it was impossible to maintain a stable pressure because of the temperature rise due to Joule heating in the solenoid windings. The apparatus is being improved and better data are expected in the near future. Nevertheless, the data points in Fig. 4 for 300 G and 1000 G show an increase of the decay rate with magnetic field.

Zeeman quenching was also observed by varying the magnetic field with the detector stationary at different positions. Figure 5 shows the falloff of the He⁻ current as a function of H^2 at three

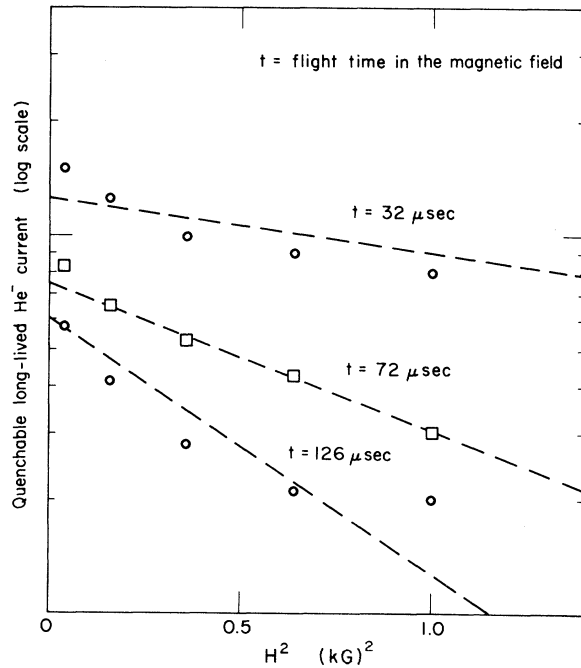


FIG. 5. Quenchable component of the He⁻ current as a function of H^2 with the detector stationary at positions corresponding to flight times of 32, 72, and 126 μ sec. At these flight times, the metastable current is due essentially only to the $J = \frac{5}{2}$ substates. One third of the zero-field $J = \frac{5}{2}$ current arises from $M_J = \pm \frac{5}{2}$, which is not quenched by Zeeman mixing and is therefore subtracted from the total current.

detector positions corresponding to flight times of 32, 76, and 126 μsec .

By the hypothesis of differential metastability, the beam should be composed of three exponential components (one for each J level) at low fields and as many as twelve components at higher fields. Our inability to resolve three distinct components deprives us of corroboration of the 4P_J state identification. However, smoothly monotonic functions of the sort shown in Fig. 3 are notoriously difficult to fit with any uniqueness by sums of exponentions. It is completely consistent with our data that the 11- μsec component is a weighted average of the $J = \frac{3}{2}$ and $J = \frac{1}{2}$ states, while the 210- μsec component is the $J = \frac{5}{2}$ state. The approximate equality of the weights of the two observed components lends support to this conclusion since the statistical weight of the $J = \frac{5}{2}$ state is equal to the sum of the weights of the $J = \frac{3}{2}$ and $\frac{1}{2}$ states. The experimental value for the weight of the short component is $45\% \pm 5\%$. If a third very short component due to, say, the $J = \frac{1}{2}$ state is produced and is lost in the distance the beam travels between production and detection, the relative weights of the two remaining components would be 40/60 in favor of the long component, a possibility we cannot rule out. On the other hand, the short component cannot be due to the $J = \frac{1}{2}$ state alone because then the weights would be 25/75 in favor of the long component. We are therefore safe in assuming that the $J = \frac{3}{2}$ lifetime, which is critical in interpreting the Zeeman quenching, is within 30% of the observed short component. Hence we will use $\gamma_{3/2} = (9 \pm 3) \times 10^4 \text{ sec}^{-1}$ in extrapolating γ_L to zero field. Future plans include an effort to determine the weights more accurately and search for a third, short-lived component in a 3000-eV beam for which the flight time to the detector is reduced to 3 μsec .

The lifetimes of the different magnetic sublevels in a magnetic field are determined by the zero-field lifetimes of the J states and Zeeman mixing coefficients. At low magnetic fields where first-order perturbation theory holds, $J = \frac{5}{2}$ mixes only with $J = \frac{3}{2}$, leading to quadratic dependence of the decay rate on H . By analogy to 3P_J in He^0 and 4P_J in Li^0 , it is expected that the $\frac{5}{2}$ - $\frac{3}{2}$ fine-structure interval is considerably greater than the $\frac{5}{2}$ - $\frac{1}{2}$ interval, and hence mixing with $J = \frac{1}{2}$ is ignored at all fields. Under the influence of a magnetic field, each M sublevel of the $J = \frac{5}{2}$ state goes over to a superposition of $J = \frac{5}{2}$ and J

$= \frac{3}{2}$ with the same M :

$$|\frac{5}{2}, M\rangle = \cos\theta_M |\frac{5}{2}, M\rangle + \sin\theta_M |\frac{3}{2}, M\rangle, \quad (1)$$

where θ_M is a function of $\mu_0 H / \Delta_{53}$ and $\Delta_{53} = \frac{5}{2} - \frac{3}{2}$ fine-structure interval. The decay rate of the modified $|\frac{5}{2}, M\rangle$ state is given by

$$\Gamma_M = \cos^2\theta_M \gamma_{5/2} + \sin^2\theta_M \gamma_{3/2}, \quad (2)$$

where $\gamma_{5/2}$ and $\gamma_{3/2}$ are the zero-field decay rates for $J = \frac{5}{2}$ and $J = \frac{3}{2}$, respectively. Because $\gamma_{3/2} \gg \gamma_{5/2}$, $\Gamma_M \geq \gamma_{5/2}$, i.e., the Zeeman mixing quenches the $J = \frac{5}{2}$ substates. At low fields, $\sin^2\theta_M$ is proportional to H^2 . In particular, $\sin^2\theta_{\pm 5/2} = 0$; the $|\frac{5}{2}, \pm \frac{5}{2}\rangle$ states remain pure at all fields. Again, because $\gamma_{3/2} \gg \gamma_{5/2}$, there is a flight time $t_0 \approx 30 \mu\text{sec}$ beyond which essentially only $J = \frac{5}{2}$ substates remain in the beam. The metastable current arising from the $J = \frac{5}{2}$ substates is then

$$I(t) = \sum_M \exp(-\Gamma_M t). \quad (3)$$

During the flight time beyond t_0 , the decay of the beam is well characterized by a single, slowly varying decay constant, γ_L . The value of γ_L at time t is equal to the logarithmic derivative of Eq. (3):

$$\gamma_L = -\frac{dI/dt}{I} = \frac{\sum_M w_M \Gamma_M}{\sum_M w_M}, \quad (4)$$

where the weights $w_M = \exp(-\Gamma_M t)$ are the relative populations of the magnetic substates after time t in the magnetic field. It is clear that γ_L first increases proportionally to H^2 , and then increases less slowly, eventually saturating, and finally decreasing to its initial value $\gamma_{5/2}$ when only $|\frac{5}{2}, \pm \frac{5}{2}\rangle$ remain in the beam. The maximum decay rate occurs at about 1000 G; hence γ_L at this field is not sensitive to changes in Δ_{53} . A better way to determine Δ_{53} , and from this the zero-field decay rate $\gamma_{5/2}$, is the direct observation of Zeeman quenching shown in Fig. 5. By Eq. (3), the $J = \frac{5}{2}$ current will drop at high fields to one-third its zero-field value. This arises from complete quenching of the $M \neq \pm \frac{5}{2}$ substates. With a flight time of 76 μsec , $I - \frac{1}{3}I_0$ drops off by a factor of e at $H = 1.06 \text{ kG}$. If $\gamma_{3/2}$ is taken to be $(9 \pm 3) \times 10^4 \text{ sec}^{-1}$, then Δ_{53} must be $(0.050 \pm 0.015) \text{ cm}^{-1}$ to produce the observed quenching. The zero-field decay rate inferred from $\Delta_{53} = (0.050 \pm 0.015) \text{ cm}^{-1}$ and a decay rate of $(4.8 \pm 0.3) \times 10^3 \text{ sec}^{-1}$ at 400 G is $\gamma_{5/2} = (2.9 \pm 0.6) \times 10^3 \text{ sec}^{-1}$ or a lifetime of $345 \pm 90 \mu\text{sec}$ for $J = \frac{5}{2}$.

These results are in apparent disagreement with the 18.2- μsec lifetime for He^- reported by

Nicholas, Trowbridge, and Allen.¹⁴ However, these investigators did not consider the differential metastability of He^- and based their conclusions on a maximum flight time of 1 μsec during which they observed a 5% decay of the beam. This agrees with the decay observed during the first microsecond of our flight time when both the short and long components are present. The 345- μsec lifetime for the $J = \frac{5}{2}$ state is in reasonable agreement with the most recent calculation of Estberg and LaBahn¹⁵ which takes into account distortion of the final state and yields a lifetime of 455 μsec . In addition, our result is in agreement with an extrapolation of the $(1s2s2p)^4P_{5/2}$ lifetimes for the He^- isoelectronic sequence from Li^0 to O^{+5} .¹⁶ The near degeneracy ($\Delta E = 0.050 \text{ cm}^{-1}$) of the $J = \frac{5}{2}$ and $J = \frac{3}{2}$ levels in He^- may be compared with the similar near degeneracy ($\Delta E = 0.070 \text{ cm}^{-1}$) of the $J = 1$ and $J = 2$ levels of the $(1s2p)^3P$ term of He^0 . The smallness of the splitting in both cases arises from competition between the spin-spin interaction and the inverted Landé spin-orbit interaction. The small value of Δ_{53} is favorable for the scheme proposed by Feldman and Novick¹⁷ for producing polarized ^3He nuclei by first obtaining a beam composed only of $|\frac{5}{2}, \pm\frac{5}{2}\rangle$ and then quenching one of the M levels by an rf resonant field.

*Work supported by the National Aeronautics and

Space Administration under Grant No. NGR-33-008-009.

¹T. Y. Wu, *Phil. Mag.* **22**, 837 (1936).

²J. W. Hilby, *Ann. Physik* **34**, 473 (1939).

³V. M. Dukel'skii, V. V. Asfrosimov, and N. V. Fedorenko, *Zh. Eksperim. i Teor. Fiz.* **30**, 792 (1956) [*Soviet Phys. JETP* **3**, 764 (1956)].

⁴P. M. Windham, P. J. Joseph, and J. A. Weinman, *Phys. Rev.* **109**, 1193 (1958).

⁵E. Holþien and J. Midtdal, *Proc. Phys. Soc. (London)* **A68**, 815 (1955).

⁶E. Holþien and S. Geltman, *Phys. Rev.* **153**, 81 (1967).

⁷B. Brehm, M. A. Gusinow, and J. L. Hall, *Phys. Rev. Letters* **19**, 737 (1967).

⁸P. Feldman, M. Levitt, and R. Novick, *Phys. Rev. Letters* **21**, 331 (1968).

⁹J. L. Pietenpol, *Phys. Rev. Letters* **7**, 64 (1961).

¹⁰C. Laughlin and A. L. Stewart, *J. Phys. B: Proc. Phys. Soc., London* **1**, 151 (1968).

¹¹S. T. Manson, *Phys. Rev.* **145**, 35 (1966), and private communication.

¹²G. N. Estberg and R. W. LaBahn, *Phys. Letters* **28A**, 420 (1968).

¹³B. L. Donnally and George Thoeming, *Phys. Rev.* **159**, 87 (1967).

¹⁴D. J. Nicholas, C. W. Trowbridge, and W. D. Allen, *Phys. Rev.* **167**, 38 (1968).

¹⁵G. N. Estberg and R. W. LaBahn, preceding Letter [*Phys. Rev. Letters* **24**, 1265 (1970)].

¹⁶P. Feldman, M. Levitt, and R. Novick, *Phys. Rev. Letters* **21**, 331 (1968).

¹⁷P. Feldman and R. Novick, in *Atomic Collision Processes*, edited by M. R. C. McDowell (North-Holland, Amsterdam, 1964), p. 201.

CROSS SECTIONS FOR INNER-SHELL VACANCY PRODUCTION IN ION-ATOM COLLISIONS*

R. C. Der, R. J. Fortner, T. M. Kavanagh, and J. M. Khan

Lawrence Radiation Laboratory, University of California, Livermore, California 94550

(Received 15 April 1970)

Cross sections for K -shell vacancy production in carbon atoms are measured for incident N^+ , O^+ , Ne^+ , and Ar^+ in various energy ranges. The measured cross sections agree with a theoretical model based on the Landau-Zener theory of level crossing.

Fano and Lichten¹ have proposed a model for inner-shell-vacancy production in ion-atom collisions. In their model, inner-shell vacancies are produced as a result of level crossings in the pseudomolecule formed during the collision. Details of the vacancy formation at a level crossing are not clear. Experimental cross sections for inner-shell-vacancy production should give information regarding the vacancy-production mechanism.

A model for the cross section has been proposed² by the authors. This model assumes that the excitation probability for inner-shell-vacancy production must follow the form of the Landau-

Zener theory.³ The cross section, based on a single level crossing, has the form

$$\sigma_I = 4\pi\alpha r_x^2 [Q_3(y/v) - Q_3(2y/v)],$$

where

$$Q_n(x) = \int_1^\infty e^{-xt} t^{-n} dt,$$

r_x is the level-crossing radius, y is a term in the Landau-Zener theory, v is the initial relative velocity of the incident ion, and α is the probability that the appropriate molecular configuration is formed.

The concept of a velocity-dependent excitation probability differs from a commonly accepted